



## **Characterization of subsurface deformation of turned brasses: Lead brass (CuZn39Pb3) and lead free brass (CuZn21Si3P)**

Downloaded from: <https://research.chalmers.se>, 2025-12-06 04:13 UTC

Citation for the original published paper (version of record):

Reddy, V., Tam, E., Krishna, A. et al (2019). Characterization of subsurface deformation of turned brasses: Lead brass (CuZn39Pb3) and lead free brass (CuZn21Si3P). Journal of Physics: Conference Series, 1183(1).  
<http://dx.doi.org/10.1088/1742-6596/1183/1/012006>

N.B. When citing this work, cite the original published paper.

PAPER • OPEN ACCESS

## Characterization of subsurface deformation of turned brasses: lead brass ( $\text{CuZn}_{39}\text{Pb}_3$ ) and lead free brass ( $\text{CuZn}_{21}\text{Si}_3\text{P}$ )

To cite this article: Vijeth V Reddy *et al* 2019 *J. Phys.: Conf. Ser.* **1183** 012006

View the [article online](#) for updates and enhancements.

### You may also like

- [On the Electrochemical Behavior and Passivation of Copper and Brass \(  \$\text{Cu}\_{70}\text{Zn}\_{30}\$  \) Electrodes in Concentrated Aqueous KOH Solutions](#)  
M. Biton, G. Salitra, D. Aurbach et al.
- [Dosimetric evaluation of hybrid brass/stainless-steel apertures for proton therapy](#)  
Hao Chen, Witold Matysiak, Stella Flampouri et al.
- [Deformation behavior in 3D molding: experimental and simulation studies](#)  
Bahador Farshchian, Alborz Amirsadeghi, Steven M Hurst et al.



The Electrochemical Society  
Advancing solid state & electrochemical science & technology

242nd ECS Meeting

Oct 9 – 13, 2022 • Atlanta, GA, US

Abstract submission deadline: **April 8, 2022**

Connect. Engage. Champion. Empower. Accelerate.

**MOVE SCIENCE FORWARD**



Submit your abstract



# Characterization of subsurface deformation of turned brasses: lead brass (CuZn<sub>39</sub>Pb<sub>3</sub>) and lead free brass (CuZn<sub>21</sub>Si<sub>3</sub>P)

Vijeth V Reddy<sup>1</sup>, Pui Lam Tam<sup>2</sup>, Amogh Vedantha Krishna<sup>1</sup> and B-G Rosén<sup>1</sup>

<sup>1</sup>Functional Surfaces Research Group, Halmstad University, Halmstad, Sweden

<sup>2</sup>Department of Industrial and Materials Science, Chalmers University of Technology, Gothenburg, Sweden

Email: vijred@hh.se

**Abstract.** The adverse effects of lead on human health and the recycling problems of copper alloys with lead content has led to the increase in concern for reducing/eliminating the use of lead in brass and other copper alloys. The real challenge prevails in sustainable manufacturing of lead free brass and to maintain as well as control the surface integrity when lead is substituted in the brass with silicon. This article is part of the study that focuses on characterizing the surface integrity of machined lead brass and lead free brass. This paper deals with the study of surface layer characteristics of brass samples, investigating the subsurface deformation influenced by the turning operation. It is important to study the plastic deformation under the machined surface which directly affects the performance of the material on further machining or application. In this study, metallographic investigations are performed on turned samples of lead brass and lead free brass and include comparisons between the study samples based on the plastic deformations quantified by grain orientations and microhardness measurements. The study performed successfully characterizes the subsurface deformation and the results suggest slightly higher subsurface deformation in turned lead brass as compared to lead free brass.

## 1. Introduction

The surface quality greatly influences the functional behaviour of a component and manufacturing efficiency and hence the study of surface integrity is an integral part in sustainable manufacturing. The addition of lead in brass greatly reduces the cutting forces and decrease in attained tool wear as compared to the lead free alternative [1]. But considering the dangerous consequences of lead contamination, manufacturing sector is increasingly focusing on identifying/ developing a contemporary manufacturing technique to increase the functionality, efficiency and to economically produce the lead free brass components. The initial investigations on surface topography of turned brass samples revealed the presence of higher surface asperities in lead brass compared to lead free brass [2].

### 1.1. Subsurface Deformation

Large temperature gradient during machining is attributed to the shear interaction between the tool and the workpiece [3]. This induces localized heating and plastic deformations in the subsurface region which may result in mechanical, thermal and metallurgical transformations [3, 4]. The surface properties of such strain hardened zones are central to the formation of wear debris [5] and accelerate corrosion [6]. These



effects in mechanical and tribological behaviour of the surface influence the functionality and efficiency of the component. The objective is to identify and evaluate the effects of machining on surface integrity of lead brass and lead free brass. In this study, turned samples of lead- and lead free brass are investigated.

Several studies [7-10] suggested machining induced strain hardening which led to higher hardness values at the near surface region below the machined surface and gradually decrease to the bulk material hardness. In this study, the plastic deformation and subsequently induced strain hardening in the subsurface are determined by the microhardness measurements. The microhardness values of lead brass and lead free brass are evaluated as a function of depth from the surface edge. Using the microhardness measurements, the depth of deformation zone for the study samples is analysed. Depth of deformation zone refers to the depth at which the hardness values attain the bulk material hardness.

Investigations [7,10,11] on the subsurface region of machined study samples suggest that the mechanical and thermal loadings during machining induce changes in microstructural attributes like grain size, orientation and dislocation density. Metallurgical alterations like elongation of grains and grain boundaries are predominantly due to plastic deformation caused by the shear forces between the tool and the workpiece during machining.

The study material's composition is listed in table 1.

**Table 1:** Chemical composition according to nominal standards (wt. %), [12][13]

Material	Cu	Zn	Pb	Si	P
CuZn <sub>39</sub> Pb <sub>3</sub> (Lead brass)	57.3	Balance	3.3	-	-
CuZn <sub>21</sub> Si <sub>3</sub> P (Lead free brass)	76	Balance	-	3	0.05

It is well known that the material's composition is critical to evaluate the effect of machining on surface integrity. Due to the compositional difference, hardness values differ between study samples with lead free brass harder than its counterpart [14]. Hence the study samples are compared by their hardness gradient with the function of depth from surface edge. The metallurgical alterations in the subsurface region are analysed using backscattered images from Scanning Electron Microscope (SEM). The grain contrast imaging using backscattered images is discernible, fast and straight-forward compared to other techniques [15].

## 2. Materials and Methods

To identify and quantify the subsurface deformation, metallographic investigations are performed on the turned lead and lead free brass samples.

### 2.1. Study samples

The study samples include cylindrical lead- and lead free brass samples subjected to turning operation using uncoated H10F cemented carbide tool primarily containing fine grain tungsten carbide with tool geometry DNGA150708F defined by ISO 1832:2012 [16] with edge radius of approx.  $10 \pm 5 \mu\text{m}$ . The samples are machined at cutting speed of 400m/min, 0.8mm depth of cut and 0.2 mm/rev feed rate.

### 2.2. Metallographic sample preparation

The samples are sectioned by wire EDM perpendicular to both the cutting direction and feed direction. The sectioned samples are mounted, as shown in figure 1, using Buehler's Konductomet™, phenolic thermoset compression mounting compound to retain the surface edge during subsequent metallographic steps. The mounted samples are ground and polished using decreasing grit size disks and low napped cloths. The cross sectional plane is etched with solution- mixture of ferric chloride (FeCl<sub>3</sub>), conc. hydrochloric acid (HCl) and distilled water in the proportion of 1:5:20. The etched samples are observed under Scanning Electron Microscope (SEM) to identify the deformation in the subsurface region.

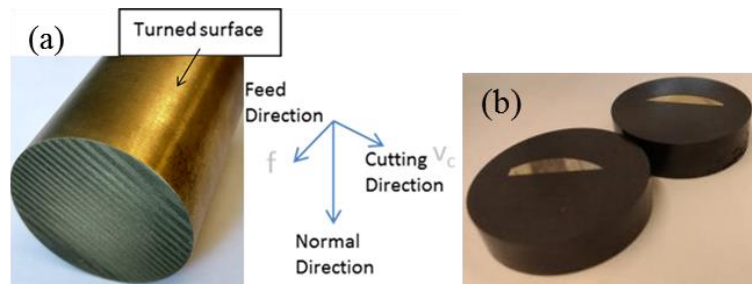


**Figure 1.** (a) Turned brass sample (b) Mounted section of brass sample

### 2.3. Vickers microhardness test

In this study, the Vickers microhardness, as specified by ISO 6507-1:2005 [17], is measured on the polished surface using the Shimadzu microhardness tester equipped with a diamond pyramid indenter. Indent load of 50g for 12 seconds is applied on the test samples in the region of interest. The measurements are taken at 10 $\mu$ m in depth and 90 $\mu$ m in lateral directions, as shown in the figure 2, with the first indent at 20  $\mu$ m from the edge due to the limitation on indenter size and indent shape acquired. Vickers microhardness test includes measuring the diagonals of the indent D1 ( $\mu$ m), D2 ( $\mu$ m) and equating in (1)

$$HV = \frac{1.8544 * F}{[(D1) * (D2)]} \quad (1)$$

Where, HV is the Vickers hardness number, F is the load applied.

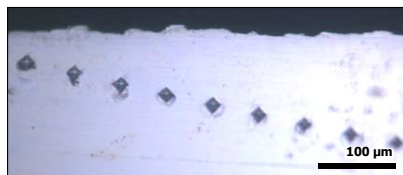


**Figure 2.** Vickers microhardness indentations

### 2.4. Grain analysis

The metallurgical alterations are analyzed using the backscattered (BSE) images of etched brass samples captured at 500X magnification with an investigation area of 250 $\mu$ m x 150 $\mu$ m. BSE detectors capture high contrast images which distinguish grains and grain boundaries. The orientation of the grains in the subsurface region is measured using Digital Surf's Mountains Map®. The image processing included binary segmentation, application of morphological filters and exclusion of incomplete grains at the borders for significant grain analysis, as shown in figure 3a. The grain orientations are the angle, as illustrated in figure 3b, by the major axis of individual grains with the horizontal plane and the average orientations are plotted as a function of depth from the surface edge.

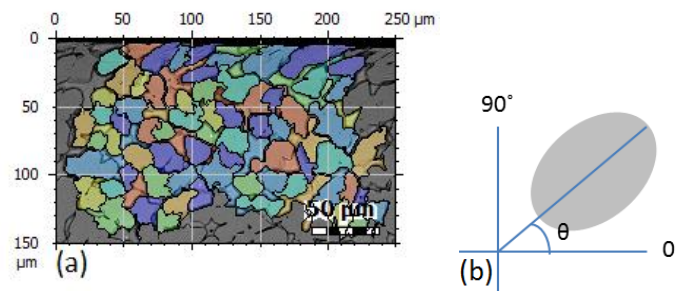


**Figure 3.** (a) Image processing in Mountains Map® (b) Illustration of grain orientation ( $\theta$ )

### 3. Results and Discussions

The backscattered electron images of lead- and lead free brass are sectioned perpendicular to the feed direction,  $f$  and cutting direction,  $v_c$  to identify and quantify the subsurface deformation.

#### 3.1. Qualitative analysis

The backscattered electron images of the subsurface region sectioned perpendicular to feed direction exhibit less- or no significant deformation in both lead- and lead free brass, as shown in figure 4, though fine grains were observed in some regions. But in the subsurface region perpendicular to the cutting direction, significant deformation exists because of higher shear in cutting direction compared to feed direction.

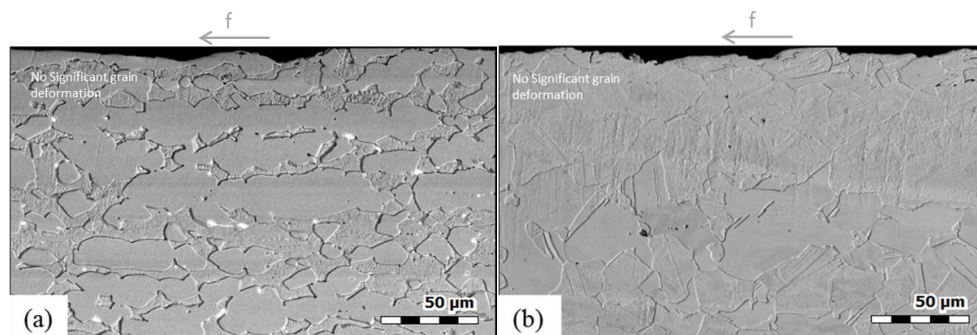


**Figure 4.** Etched subsurface region of (a) lead brass and (b) lead free brass samples sectioned perpendicular to the feed direction,  $f$

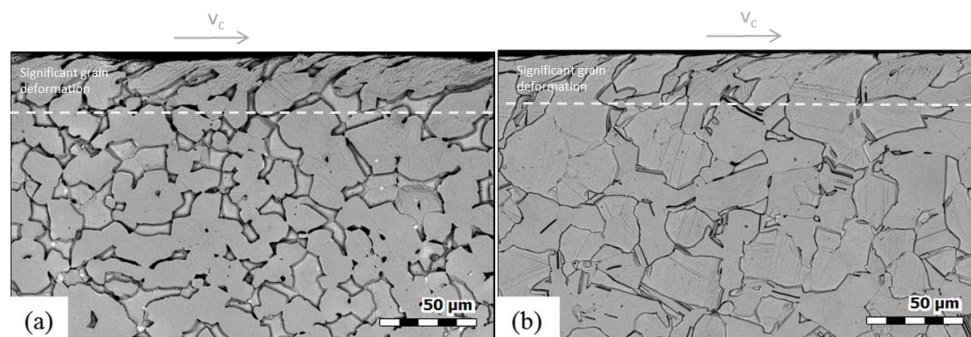


**Figure 5.** Etched subsurface region of (a) lead brass and (b) lead free brass samples sectioned perpendicular to the cutting direction,  $v_c$ . The delineated line approximately separates the deformed grain with the bulk material

In general, the grains are distributed randomly but in the region just beneath the machined surface perpendicular to direction of cut, non-randomness in orientation of grains exists. The grain and grain boundaries are elongated and oriented in the direction of cut, as shown in figure 5. The unaltered region further below is the bulk material zone which is unaffected by the machining conditions.

### 3.2. Quantitative analysis

Vickers microhardness measurements and grain orientation analysis are performed to quantify the depth and intensity of subsurface deformation.

**3.2.1. Microhardness measurements.** Vickers microhardness test was conducted on the study samples. The ploughing phenomenon of turning operation induces strain hardening in the near surface region which results in higher hardness values. From the figure 6, it is evident that the hardness values are higher near to the surface and gradually reduces reaching the bulk hardness.

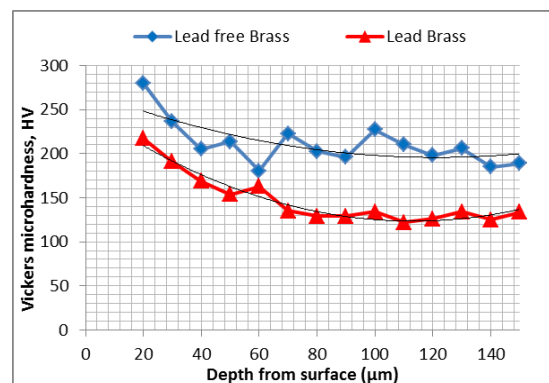


**Figure 6.** Vickers microhardness measurements

The hardness values of lead brass and lead free brass reach the bulk hardness values at approximately 80μm and 60μm respectively. Comparing the gradient of hardness values, higher hardness is induced by machining in lead brass compared to lead free brass.

**3.2.2. Grain orientation.** The average orientation of grains from image grid size 10μm x 250μm to 150μm x 250μm with an incremental size of 10μm in depth are measured and plotted as a function of depth from the surface. As earlier discussed, the grains are oriented randomly and even out to approximately 90 degrees in the bulk material zone. But the grains in the subsurface region of machined surface progressively orient towards the direction of cut and almost become parallel to the surface edge. The plots in figure 7 represent the grain orientation angle ( $\theta$ ) of lead- and lead free brass plotted as the function of depth from surface edge. The machining induced grain orientations are higher near the surface edge and lower in the region of bulk material.



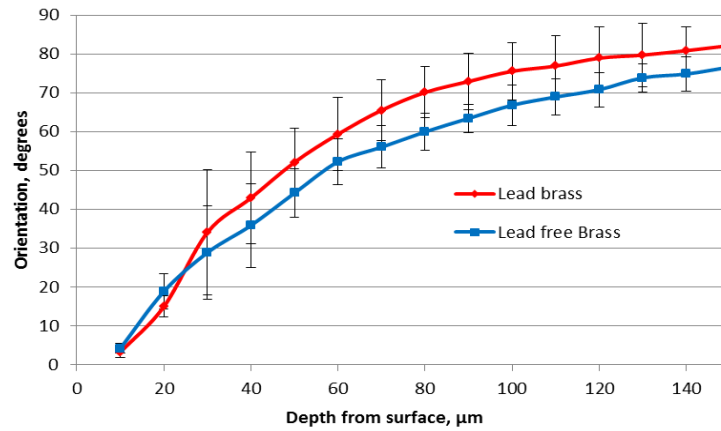


**Figure 7.** Variation of grain orientation of study samples as function of depth from surface edge

Further, the grain orientation angles are used to study the strain induced in the subsurface. Few investigations [18,19] on the flow lines in the subsurface region in a sliding test, estimated the equivalent strain,  $\epsilon_{eq}$ , using the angle made by the flow lines as a function of depth from surface edge. CA Brown [20] calculated the strain induced in machined chips from the grain elongations. Similarly in this study, grain orientations in the subsurface region from ploughing effect of turning operation are used to calculate the equivalent strain,  $\epsilon_{eq}$ , from (2).

$$\epsilon_{eq} = \frac{\sqrt{3}}{3} \tan(90 - \theta) \quad (2)$$

Where,  $\theta$  is the grain orientation angle

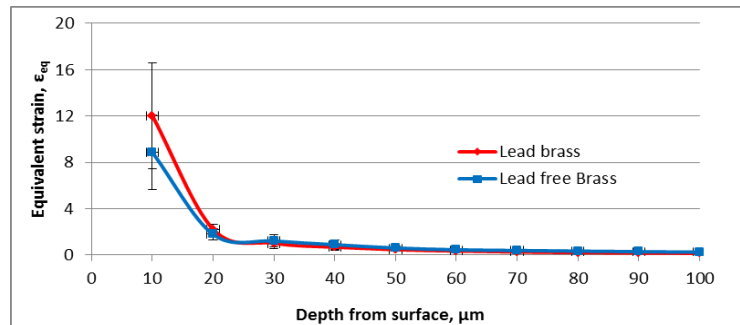


**Figure 8.** Equivalent strain as a function of depth from surface, calculated with mean grain orientations.

From figure 8, it is evident that the estimated plastic strain induced is higher in the subsurface region of study samples and the differences in the intensity of plastic strain in lead brass is marginal compared to lead free brass.

**3.2.3. Underlying mechanism.** Lead brass offers lower cutting forces at the tool/work interface, primarily due to the presence of lead, and as a result generates discontinuous chips, whereas lamellar chips are generated while machining lead free brass [1,13]. The formation of discontinuous chips while machining lead brass, due to lower tool forces, causes a ripping effect on the workpiece surface [21]. This ripping effect induces slightly higher roughness and additional strain than normal cutting effect on the lead brass surface.



#### 4. Conclusion

The results and analysis are specific to the study samples and machining conditions. The following conclusions can be drawn from the study:

1. Vickers microhardness measurements suggest turning operation influence strain hardening in the subsurface region of the brass samples with higher induced hardness in lead brass.
2. The grain analysis suggest significant metallurgical alterations observed in the subsurface region perpendicular to the direction of cut and very little or insignificant grain deformation observed in the region perpendicular to the feed direction.
3. From the grain orientation analysis, effective strain is estimated and the differences in the plastic strain between the lead brass and lead free brass are found to be marginal.
4. Considering the hardness measurements and equivalent strain, intensity of subsurface deformation in turned lead free brass is in proximity with turned lead brass samples.

Therefore the study results suggest the possibility to attain subsurface characteristics of lead brass by replacing the lead content with silicon. Future work includes multi-scale investigations on subsurface region by comparing the results of grain orientations using electron microscopy with the crystal misorientation using Electron Back Scattered Diffraction (EBSD) technique.

#### Acknowledgment

The research presented in this paper is a part of the Lead Free Brass research project funded by MISTRA (the Swedish Foundation for Strategic Environmental Research), and SIO (the Swedish Strategic Innovation Area). The authors would like to thank; AB Markaryds Metallarmatur, Markaryd for their participation in this project; Digital Surf for providing us the software MountainsMap® Premium and all colleagues in the Functional Surfaces Research Group at Halmstad University for their help, support and cooperation.

#### References

- [1] Trent E and P Wright 2000 *Metal Cutting: Fourth edition* Butterworth Heinemann Stoneham MA USA
- [2] Vijeth V Reddy, Amogh Vedantha Krishna, Fredrik Schultheiss and B-G Rosén 2017 Surface Topography Characterization of Brass Alloys: Lead Brass (CuZn39Pb3) and Lead free Brass (CuZn21Si3P) Surf. Topogr.: Metrol. Prop. 5 025001 <https://doi.org/10.1088/2051-672X/aa612b>
- [3] Guy Bellows, Dean N. Tishler 1970 Introduction to Surface Integrity General Electric Aircraft Engine Group Cincinnati Ohio
- [4] V. I. Levitas, V. F. Nesterenko and M. A. Meyers 1998 Strain-Induced Structural Changes and Chemical Reactions Part II Acta materialia USA
- [5] S.L. Rice, H. Nowotny, S.F. Wayne 1989 A Survey of the Development of Subsurface Zones in the Wear of Materials Key Engineering Materials Vol. 33 pp. 77-100
- [6] D. Landolt, S. Mischler, M. Stemp, S. Barril 2004 Third Body Effects and Material Fluxes in Tribocorrosion Systems Involving a Sliding Contact Wear Volume 256 Issue 5 Pages 517-524 ISSN 0043-1648 [http://dx.doi.org/10.1016/S0043-1648\(03\)00561-1](http://dx.doi.org/10.1016/S0043-1648(03)00561-1)
- [7] A. Moshkovich, V. Perfilyev, I. Lapsker, D. Gorni, L. Rapoport 2011 The Effect of Grain Size on Stribeck Curve and Microstructure of Copper Under Friction in the Steady Friction State Tribology Letters 42 pp. 89-98
- [8] A. Thakur, S. Gangopadhyay, K.P. Maity 2014 Effect of Cutting Speed and Tool Coating on Machined Surface Integrity of Ni-based Super Alloy Procedia CIRP Volume 14 Pages 541-545 ISSN 2212-8271 <http://dx.doi.org/10.1016/j.procir.2014.03.045>
- [9] Mike Olsson, Volodymyr Bushlya, Jinming Zhou, Jan-Eric Ståhl 2016 Effect of Feed on Sub-surface Deformation and Yield Strength of Oxygen-free Pitch Copper in Machining Procedia CIRP Volume 45 Pages 103-106 ISSN 2212-8271 <http://dx.doi.org/10.1016/j.procir.2016.02.163>

- [10] Z. Pan, Y. Feng, S.Y. Liang 2017 Material Microstructure Affected Machining: a Review Manufacturing Review 4 p. 5
- [11] Fergani O, Liang SY 2015 The Effect of Machining Process Thermo-Mechanical Loading on Workpiece Average Grain Size Int J Adv Manuf Technol 80:21–29 doi:10.1007/s00170-015-6975-8
- [12] Wieland-SW1 Lead-free Special Brass Wieland-Werke AG [www.wieland.de](http://www.wieland.de) 2014-01-28
- [13] Wieland-Z32/Z33 Machining Brass Wieland-Werke AG [www.wieland.de](http://www.wieland.de) 2014-01-28
- [14] Schultheiss F, Lundström E, Johansson D, Bushlya V, Zhou J, Nilsson K and Ståhl J-E 2014 Machinability of Lead-Free Brass—a Comparative Study Swedish Prod. Symp
- [15] Canovic S, Jonsson T, Halvarsson M 2008 Grain Contrast Imaging in FIB and SEM Institute Phys. Conf. Series vol. 126 pp 012054
- [16] ISO 1832:2012 2012–11 Indexable inserts for cutting tools—designation (International Organization for Standardization)
- [17] ISO 6507-1:2005 Metallic materials -- Vickers hardness test -- Part 1: Test method
- [18] Dautzenberg. J. H & Zaat J. H 1973 Quantitative Determination of Deformation by Sliding Wear Wear 23(1) 9-19 DOI: 10.1016/0043-1648(73)90036-7
- [19] Pradeep L. Menezes, Kishore, Satish V. Kailas 2009 Role of Surface Texture of Harder Surface on Subsurface Deformation Wear Volume 266 Issue 1 Pages 103-109 ISSN 0043-1648 <http://dx.doi.org/10.1016/j.wear.2008.05.008>
- [20] C.A. Brown 1987 Strain Analysis in Machining using Metallographic Methods Metallography Volume 20 Issue 4 Pages 465-483 ISSN 0026-0800 [http://dx.doi.org/10.1016/0026-0800\(87\)90020-6](http://dx.doi.org/10.1016/0026-0800(87)90020-6)
- [21] Toenshoff H K and Denkena B 2013 Basics of Cutting and Abrasive Processes (Berlin: Springer)